Freight derivatives pricing for decoupled mean-reverting diffusion and jumps

Ioannis Kyriakou*, Panos K. Pouliasis†,
Nikos C. Papapostolou‡and Kostas Andriosopoulos§

Abstract

We develop an accurate valuation setup for freight options, featuring an exponential mean-reverting model for the freight rate with distinct reversion scales for its jump and diffusion components. We calibrate to Baltic option prices and analyze the freight rate dynamics. More specifically, we observe that jumps dissipate faster than the diffusive deviations about the equilibrium level. We benchmark against practitioners' model of choice, i.e., the lognormal model and variants, and find that our approach reduces the pricing error while preserving analytical tractability and computational competence. We also find that neglecting fast mean-reverting jumps leads to nontrivial option mispricings.

Key words: uncertainty modelling; ocean freight; estimation; freight derivatives; pricing

*Cass Business School, City, University of London, 106 Bunhill Row, London EC1Y 8TZ, UK. Email: ioannis.kyriakou@city.ac.uk.

†Cass Business School, City, University of London, 106 Bunhill Row, London EC1Y 8TZ, UK. Email: p_pouliasis@city.ac.uk.

‡Cass Business School, City, University of London, 106 Bunhill Row, London EC1Y 8TZ, UK. Email: n.papapostolou@city.ac.uk.

§Corresponding author. ESCP Europe Business School, 527 Finchley Road, London NW3 7BG, UK. Email: kandriosopoulos@escpeurope.eu.

1 Introduction

The evolution of modelling, operations management, and optimization techniques has transformed the shipping industry and various sectors have been restructured to take advantage of these innovations. Inevitably, these advancements affected also the bulk sector, an important sector of the world economy[1], that demonstrated gradual revamping and utilization of newly developed tools aiming to appropriately capture the realism of a market characterized by uncertainty of future economic conditions and sluggish supply adjustment to changes in demand due to time-to-build lags, implying the need for sufficiently sophisticated approaches in shipping asset valuation.

In recent years, the trading volume of contingent claims in the market has grown rapidly. Kavussanos and Visvikis (2004) found that the introduction of freight derivatives trading decreased the price volatility, had an impact on its asymmetry, and improved the speed of information flow in freight markets. Options have gained acceptance as invaluable tools among market participants, not only for hedging physical exposures, but also for providing investors with versatility, including several expiration dates available for trading, as well as the ability to leverage and trade volatility. Freight derivative markets lack the liquidity of equity and conventional commodity markets, but this is now changing with the increasing participation of investment banks and hedge funds, in addition to traditional physical players such as shipowners, operators and trading houses. Alizadeh et al. (2015) have assessed the existence of liquidity risk and reported that this is priced and plays an important role in Forward Freight Agreement (FFA) returns. Moreover, freight forward/futures prices have been found to informationally lead the underlying freight rates (e.g., Kavussanos and Visvikis, 2004) and lag the commodity futures prices (Kavussanos et al., 2014). Alexandridis et al. (2017) have examined the spillover effects of time-charter rates, freight futures and options prices, and their association with trading activities and market liquidity of freight futures contracts; they have found significant information transmission in both returns and volatilities among the three markets.

In 2015, the equivalent trading volume in FFAs was approximately 640,000 cargo trading days, which was roughly equivalent to the full capacity of the underlying capesize fleet. The option market also appeared popular with a trading volume of 280,000 cargo days for 2015 and an average weekly open interest of 140,000 cargo trading days (source: www.balticexchange.com).

[1]With over 80% of world merchandise trade being carried by sea, maritime transportation remains the backbone of international trade and a leading indicator of the global economy, which explains why the particular industry has attracted much interest in the finance literature (see Kilian, 2009, Kalouptsidi, 2014, Papapostolou et al., 2014, Greenwood and Hanson, 2015).

Therefore, it is not surprising that the valuation and hedging of freight contingent claims have received attention from practitioners and researchers (see, for example, Koekebakker et al., 2007, Jørgensen and De Giovanni, 2010, Prokopczuk, 2011, Nomikos et al., 2013), especially from 2008 onwards; a period which was characterized by a notoriously high volatility.

Freight rates exhibit properties that distinguish them from other markets. Such are, for example, the high volatility, mean-reversion/cyclical behavior of rates and prices, and the non-storability of freight rates (e.g., see Kavussanos and Visvikis, 2006). Geman and Smith (2012) demonstrate that freight rate trajectories differ not only from traditional assets, such as stocks and bonds, but also from most commodities; electricity is a market that shares similar stylized empirical facts, such as absence of storability and high volatility. Maritime economic theory stipulates that, in a competitive freight market, rates are reverting[2] to long-run costs (Zannetos, 1966, Koekebakker et al., 2006). Poor market conditions and low freight rates halt investment in shipping projects, reducing eventually the supply of vessels due to increased demolition activity in a stagnant market (where excess tonnage is laid up). On the other hand, prosperous market conditions provide disincentives to scrapping and encourage new orders. Inevitably, new vessel deliveries shift gradually the supply curve to the right, putting downward pressure to freight rates. Consistently with this, several authors argue that mean-reversion is supported in freight rates. For example, Bjerksund and Ekern (1995) and Jørgensen and De Giovanni (2010) assume a Gaussian Ornstein–Uhlenbeck process for the spot freight rate, which, nevertheless, is not downward-restricted implying possible negative spot freight rates, especially when volatility is high, and is inconsistent with empirical facts about actual rates such as skewness. These deficiencies can be alleviated by using an exponential mean-reverting process as in Tvedt (1997, 2003). Adland and Cullinane (2006), instead, propose a non-parametric diffusion model for the freight rate dynamics in the tanker markets, which allows them to bypass potential parametric restrictions by estimating the drift and diffusion functions non-parametrically. More recently, focusing on Supramax spot rates, Benth and Koekebakker (2016) find evidence of volatility clustering and long-range memory effect, which they try to capture by means of a combined autoregressive with stochastic volatility model approach.

Another salient feature of freight rates is that of extreme price movements. Price discontinuities

[2]These models have been used extensively in the commodity literature to account for supply and demand fundamentals that induce reversion to some equilibrium level as commodity prices tend to fluctuate about values determined by the marginal cost of production; see, for example, the seminal papers by Bessembinder et al. (1995) and Schwartz (1997).

are observed during periods of tight supply and demand schedules due to the inability of supply to immediately respond to increased demand for seaborne transportation. Downside movements are also remarkable: for example, during the period 2003–2008, freight rates for capesize dry bulk carriers, with a cargo-carrying capacity of 180,000 mt dwt, increased from an average rate of 20,000 USD/day to a maximum of 236,000 USD/day only to drop to 6,000 USD/day within a period of four months after the onset of the financial crisis. Nevertheless, simply modelling freight rates using a classical diffusion model overlaid with jumps of normal size (Merton model, see Nomikos et al., 2013) results in jump shocks persisting for prolonged periods of time; the importance of additionally incorporating mean-reversion has been emphasized, for example, in Geman and Roncoroni (2006) when modelling power prices.

The purpose of this paper is to study the freight model with decoupled mean-reverting diffusive and jump components with distinct reversion scales, for the two largest in size dry bulk carriers, i.e., capesize and panamax, reflecting freight's distinctive self-adjustment behaviour under tight and ordinary supply-demand patterns. We have seen previous use of such model construction in offshore shipping markets (Bjørkelund, 2014) with limited empirical application, though, due to inexistent derivatives' market for the offshore segment, but also in energy markets (e.g., see Hikspoors and Jaimungal, 2007 and Nomikos and Soldatos, 2008). Our contribution lies in deriving a relevant analytical formula for tradable average options and calibrating to market quotes of Baltic Capesize Index (BCI) and Baltic Panamax Index (BPI) options that are prevalent in the dry bulk market. By means of sensitivity analyses, we compare against simpler model constructions without jumps and/or two-regime mean-reversion, which market practitioners seem to have favoured so far due to their simplicity and analytical tractability. While maintaining these two desired features under the more sophisticated spot model proposed, we demonstrate its ability to reproduce stylized features of freight rates in the dry bulk sector. Our analysis of option pricing error statistics shows that the postulated model generates lower error than the basic lognormal. Moreover, a regression analysis shows that superimposing jumps on the spot rate diffusion improves on the option pricing biases.

The remainder of the paper is organized as follows. In Section 2, we present our spot and option price models. In Sections 3 and 4, we introduce our option data set and estimation procedure, whereas in Section 5, we perform our model validation and discuss the outcome from the empirical

estimation of model parameters, analyze the option pricing errors, and compare with various nested models. Section 6 concludes.

2 Model setting

2.1 Spot price model

Let S_t denote the spot freight rate at time t. We decompose S_t into two independent stochastic factors,

$$\ln S_t = X_t + Y_t, \tag{1}$$

where X is assumed to revert towards ε following the Gaussian Ornstein–Uhlenbeck process

$$dX_t = k_1(\varepsilon - X_t)dt + \sigma dW_t,$$

and the jump process Y is represented by the mean-reverting Lévy-driven model

$$dY_t = -k_2 Y_t dt + dL_t.$$

Here W is a standard Brownian motion and L a time-homogeneous compound Poisson process. In particular, the diffusion component of the log-price reverts to level ε at rate k_1 and has volatility σ, whereas jumps of random size J arrive subject to constant rate λ and dissipate at rate k_2. J is modelled by a sequence of independent and identical normal random variables with $E(J) =: \mu_J$ and $\mathrm{Var}(J) =: \sigma_J^2$.

The characteristic function of (1) is given by

$$\phi(u;t) := E\left(e^{iu\ln S_t}\right) = e^{iu(X_0 e^{-k_1 t} + Y_0 e^{-k_2 t}) + iu\varepsilon(1-e^{-k_1 t}) - \frac{1}{4k_1}\sigma^2 u^2(1-e^{-2k_1 t}) + \int_0^t \xi(ue^{k_2(s-t)})ds}, \tag{2}$$

where

$$\xi(u) := \ln E(e^{iuL_1}) = \lambda(e^{iu\mu_J - \frac{1}{2}u^2\sigma_J^2} - 1)$$

is the characteristic exponent of L. The cumulants of $\ln S_t$ follow from

$$c_k = \frac{1}{i^k}\frac{\partial^k \ln\phi}{\partial u^k}(0;t)$$

and are explicitly given by

$$c_1 = E(\ln S_t) = e^{-k_1 t}(X_0 - \varepsilon) + \varepsilon + e^{-k_2 t}\left(Y_0 - \frac{\lambda\mu_J}{k_2}\right) + \frac{\lambda\mu_J}{k_2}, \tag{3}$$

$$c_2 = \mathrm{Var}(\ln S_t) = \frac{\sigma^2(1-e^{-2k_1 t})}{2k_1} + \frac{\lambda(\mu_J^2+\sigma_J^2)(1-e^{-2k_2 t})}{2k_2}, \tag{4}$$

$$c_3 = E\left[(\ln S_t - E(\ln S_t))^3\right] = \frac{\lambda\mu_J(\mu_J^2+3\sigma_J^2)(1-e^{-3k_2 t})}{3k_2}, \tag{5}$$

$$c_4 = E\left[(\ln S_t - E(\ln S_t))^4\right] - 3\mathrm{Var}^2(\ln S_t) = \frac{\lambda(\mu_J^4+6\mu_J^2\sigma_J^2+3\sigma_J^4)(1-e^{-4k_2 t})}{4k_2}. \tag{6}$$

Note that as the forecast horizon increases (i.e., $t \to \infty$), the terms $\exp(-k_1 t)$, $\exp(-k_2 t)$, $\exp(-2k_2 t)$, $\exp(-3k_2 t)$, $\exp(-4k_2 t)$ approach zero and the cumulants of the log-spot price approach, respectively, $\varepsilon+\lambda\mu_J/k_2$, $\sigma^2/(2k_1)+\lambda(\mu_J^2+\sigma_J^2)/(2k_2)$, $\lambda\mu_J(\mu_J^2+3\sigma_J^2)/(3k_2)$ and $\lambda(\mu_J^4+6\mu_J^2\sigma_J^2+3\sigma_J^4)/(4k_2)$. Scale-free versions of the third and fourth cumulants, i.e., the skewness coefficient and excess kurtosis, are given respectively by

$$\frac{c_3}{c_2^{3/2}} \quad \text{and} \quad \frac{c^4}{c_2^2}. \tag{7}$$

In the rest of this paper, we will dub the dynamics of the spot price S defined through (1) as the MR2JD (exponential 2-regime mean-reverting jump diffusion) model. The model encompasses as special cases the:

MRJ: exponential mean-reverting jump diffusion model with a common decay rate for the jumps and diffusion ($k_2 = 0$);

MR: exponential Gaussian Ornstein–Uhlenbeck model without jumps ($k_2 = 0$, $dL_t = 0$ for all t);

LGN: lognormal (exponential Gaussian) model without jumps and mean-reversion.

2.2 FFA model

A future arithmetic average of the spot S consists of n fixings at time points $t_1 < t_2 < \cdots < t_n$. The FFA is a cash-settled financial contract that gives its owner the difference between the average and the price F_{0,t_1,t_n}. As the cost of entering the FFA is nil, F_{0,t_1,t_n} has to satisfy the expected present value equation

$$E\left[e^{-rT}\left(\frac{1}{n}\sum\nolimits_{j=1}^{n} S_{t_j} - F_{0,t_1,t_n}\right)\right] = 0,$$

from which the FFA price is given by the average expected spot price

$$F_{0,t_1,t_n} = \frac{1}{n}\sum\nolimits_{j=1}^{n} E(S_{t_j}) = \frac{1}{n}\sum\nolimits_{j=1}^{n} \phi(-i; t_j), \tag{8}$$

where the second equality follows from (2).

2.3 Option price model

The arithmetic average-based settlement procedure for freight options is inherited from the FFA market. Their importance is attributed to their ability to mitigate problems relating to market manipulation of the underlying freight prior or during to settlement, especially in such thinly traded markets. More specifically, suppose that the spot price S is monitored over the period $[\tau, T]$, $T > \tau \geq 0$, at the following equidistant dates: $\tau, \tau+\delta, \ldots, \tau+j\delta, \ldots, \tau+n\delta = T$. In the case of the freight option, the arithmetic average of the $n+1$ spot prices up to the option maturity T,

$$\frac{1}{n+1}\sum\nolimits_{j=0}^{n} S_{\tau+j\delta},$$

settles against a fixed strike price K. The price of the option then reads

$$E\left[e^{-rT}\left(\frac{1}{n+1}\sum\nolimits_{j=0}^{n} S_{\tau+j\delta} - K\right)^{+}\right], \tag{9}$$

where $x^{+} := \max(x, 0)$ and $r \geq 0$ is the continuously compounded risk free rate of interest. Note that for $\tau = 0$ the period to maturity and the averaging period coincide, i.e., both are equal to T; in the case of a *forward start* option, the commencement of averaging is deferred to the predetermined future time $\tau > 0$ and is completed at T, i.e., the time to maturity of the option T is greater than the length of the averaging period $T - \tau > 0$.

It is a well-established fact that, in general, the expectation (9) cannot be given in closed form. Our goal is to provide a very sharp proxy for its value in a way that allows retaining the advantages of closed-form formulae, i.e., high accuracy and computational speed. To this end, it is necessary to define first the random variables

$$Z_j = X_{\tau+j\delta} - X_{\tau+(j-1)\delta}e^{-k_1\delta},\ \Psi_j = Y_{\tau+j\delta} - Y_{\tau+(j-1)\delta}e^{-k_2\delta} \tag{10}$$

for $1 \leq j \leq n$, and

$$Z_0 = X_\tau - X_0 e^{-k_1 \tau},\ \Psi_0 = Y_\tau - Y_0 e^{-k_2 \tau}, \tag{11}$$

with characteristic functions

$$\varphi_Z(u;t) := E\left(e^{iuZ}\right) = e^{iu\varepsilon(1-e^{-k_1 t}) - \frac{1}{4k_1}\sigma^2 u^2 (1-e^{-2k_1 t})}, \tag{12}$$

$$\varphi_\Psi(u;t) := E\left(e^{iu\Psi}\right) = e^{\int_0^t \xi(ue^{k_2(s-t)})ds}. \tag{13}$$

From the decomposition $\ln S = X + Y$ (see Eq. 1) and Eqs. (10)–(11), we get by recursive substitution that

$$\ln S_{\tau+j\delta} = X_0 e^{-k_1(\tau+j\delta)} + Y_0 e^{-k_2(\tau+j\delta)} + \sum_{m=0}^{j} (Z_m e^{-(j-m)k_1\delta} + \Psi_m e^{-(j-m)k_2\delta}), \tag{14}$$

from which

$$\begin{aligned} \sum_{j=0}^{n} \ln S_{\tau+j\delta} &= \sum_{j=0}^{n} \left(X_0 e^{-k_1(\tau+j\delta)} + Y_0 e^{-k_2(\tau+j\delta)}\right) + \sum_{j=0}^{n} \left(Z_j \sum_{m=0}^{n-j} e^{-mk_1\delta} + \Psi_j \sum_{m=0}^{n-j} e^{-mk_2\delta}\right) \\ &= C_{1,0} X_0 e^{-k_1\tau} + C_{2,0} Y_0 e^{-k_2\tau} + \sum_{j=0}^{n} \left(C_{1,j} Z_j + C_{2,j} \Psi_j\right), \end{aligned} \tag{15}$$

where

$$C_{l,j} := \frac{e^{k_l\delta} - e^{-k_l(n-j)\delta}}{e^{k_l\delta} - 1},\ l = 1, 2.$$

Based on these preliminaries, we prove the following result which forms the main premise of our approach to evaluating (9); we state it as a proposition for future reference.

Proposition 1. *The characteristic function of the pair* $(\ln S_{\tau+w\delta}, \sum_{j=0}^{n} \ln S_{\tau+j\delta}/(n+1))$ *for any*

$0 \leq w \leq n$ *is given by*

$$\begin{aligned}
\Phi_w(u,\upsilon) &= E\left[\exp\left(iu\ln S_{\tau+w\delta} + \frac{i\upsilon}{n+1}\sum_{j=0}^{n}\ln S_{\tau+j\delta}\right)\right] \\
&= \exp\left[iX_0\left(ue^{-k_1(\tau+w\delta)} + \frac{\upsilon C_{1,0}e^{-k_1\tau}}{n+1}\right) + iY_0\left(ue^{-k_2(\tau+w\delta)} + \frac{\upsilon C_{2,0}e^{-k_2\tau}}{n+1}\right)\right] \\
&\quad \times\varphi_Z\left(ue^{-wk_1\delta} + \frac{\upsilon C_{1,0}}{n+1};\tau\right)\varphi_\Psi\left(ue^{-wk_2\delta} + \frac{\upsilon C_{2,0}}{n+1};\tau\right) \\
&\quad \times\prod_{j=1}^{w}\varphi_Z\left(ue^{-(w-j)k_1\delta} + \frac{\upsilon C_{1,j}}{n+1};\delta\right)\varphi_\Psi\left(ue^{-(w-j)k_2\delta} + \frac{\upsilon C_{2,j}}{n+1};\delta\right) \\
&\quad \times\prod_{j=w+1}^{n}\varphi_Z\left(\frac{\upsilon C_{1,j}}{n+1};\delta\right)\varphi_\Psi\left(\frac{\upsilon C_{2,j}}{n+1};\delta\right). \qquad (16)
\end{aligned}$$

Proof. From (14)–(15) and for $0 \leq w \leq n$,

$$\begin{aligned}
&\exp\left(iu\ln S_{\tau+w\delta} + \frac{i\upsilon}{n+1}\sum_{j=0}^{n}\ln S_{\tau+j\delta}\right) \\
&= \exp\left[iu\left(X_0e^{-k_1(\tau+w\delta)} + Y_0e^{-k_2(\tau+w\delta)}\right) + \frac{i\upsilon}{n+1}\left(C_{1,0}X_0e^{-k_1\tau} + C_{2,0}Y_0e^{-k_2\tau}\right)\right] \\
&\quad \times\exp\left[iu\sum_{j=0}^{w}(Z_je^{-(w-j)k_1\delta} + \Psi_je^{-(w-j)k_2\delta}) + \frac{i\upsilon}{n+1}\sum_{j=0}^{n}(C_{1,j}Z_j + C_{2,j}\Psi_j)\right] \\
&= \exp\left[iX_0\left(ue^{-k_1(\tau+w\delta)} + \frac{\upsilon C_{1,0}e^{-k_1\tau}}{n+1}\right) + iY_0\left(ue^{-k_2(\tau+w\delta)} + \frac{\upsilon C_{2,0}e^{-k_2\tau}}{n+1}\right)\right] \\
&\quad \times\exp\left\{i\sum_{j=0}^{w}\left[Z_j\left(ue^{-(w-j)k_1\delta} + \frac{\upsilon C_{1,j}}{n+1}\right) + \Psi_j\left(ue^{-(w-j)k_2\delta} + \frac{\upsilon C_{2,j}}{n+1}\right)\right]\right. \\
&\quad \left. + \frac{i\upsilon}{n+1}\sum_{j=w+1}^{n}(C_{1,j}Z_j + C_{2,j}\Psi_j)\right\}. \qquad (17)
\end{aligned}$$

Result (16) then follows by taking the expectation of (17) and making use of the stochastic independence of the random variables $\{Z_j\}$ and $\{\Psi_j\}$ defined in (10)–(11) with characteristic functions (12)–(13). □

Contrary to the case of the FFA (see Section 2.2), the main obstruction to a closed-form formula for the expected value (9) is the nature of the exercise region of the option together with the lack of knowledge of the distribution law of the arithmetic average. We will derive our pricing formula from a set of lower bounds for the option price. To this end, we will replace the exercise region by an

alternative region that will bring more analytical tractability and lead to a lower bound. As to the choice of this region, we will follow Curran (1994), Rogers and Shi (1995) and Fusai and Kyriakou (2016):

$$\mathrm{LB}(l) := E\left[e^{-rT}\left(\frac{1}{n+1}\sum\nolimits_{j=0}^{n} S_{\tau+j\delta} - K\right)\mathbf{1}_{\left\{\frac{1}{n+1}\sum_{j=0}^{n}\ln S_{\tau+j\delta} > l\right\}}\right]. \tag{18}$$

Varying the free parameter l in (18) leads to different lower bounds; we will denote by l^* the maximizer of (18):

$$l^* = \arg\max_{l} \mathrm{LB}(l).$$

The option price will be given by the optimal lower bound presented in Proposition 2 using the results developed in Proposition 1 as a means for translating the option price into a Fourier-transform representation in terms of explicit characteristic functions which retains the speed-accuracy advantages of a true closed-form formula.

Proposition 2. *The optimal lower bound is given by*

$$\mathrm{LB}(l^*) = \frac{e^{-\delta l^* - rT}}{2\pi}\int_{\mathbb{R}} \frac{e^{-iul^*}}{iu+\delta}\left(\frac{1}{n+1}\sum_{j=0}^{n}\Phi_j(-i, u-i\delta) - K\Phi_n(0, u-i\delta)\right)du, \tag{19}$$

where constant $\delta > 0$ ensures integrability, and l^* is the solution of

$$\int_{\mathbb{R}} e^{-il^*\upsilon}\left(\sum_{j=0}^{n}\Phi_j(-i,\upsilon) - K(n+1)\Phi_n(0,\upsilon)\right)d\upsilon = 0 \tag{20}$$

with Φ given by (16).

Proof. The Fourier transform of the lower bound (18) with respect to l is well-defined upon introducing the exponential dampening factor $e^{\delta l}$ with $\delta > 0$ and is given by

$$\frac{e^{-rT}}{n+1}\int_{\mathbb{R}} e^{iul+\delta l}\sum_{j=0}^{n} E\left[\left(S_{\tau+j\delta} - K\right)\mathbf{1}_{\left\{\frac{1}{n+1}\sum_{j=0}^{n}\ln S_{\tau+j\delta} > l\right\}}\right]dl.$$

Applying Fubini's theorem yields

$$\begin{aligned}
&\frac{e^{-rT}}{n+1}\sum_{j=0}^{n} E\left[(S_{\tau+j\delta}-K)\int_{-\infty}^{\frac{1}{n+1}\sum_{j=0}^{n}\ln S_{\tau+j\delta}} e^{i(u-i\delta)l}dl\right] \\
= \;& \frac{e^{-rT}}{iu+\delta}\left[\frac{1}{n+1}\sum_{j=0}^{n} E\left(e^{\ln S_{\tau+j\delta}+\frac{i(u-i\delta)}{n+1}\sum_{j=0}^{n}\ln S_{\tau+j\delta}}\right) - KE\left(e^{\frac{i(u-i\delta)}{n+1}\sum_{j=0}^{n}\ln S_{\tau+j\delta}}\right)\right].
\end{aligned}$$

Then, given the definition (16), (19) follows by standard Fourier inversion (e.g., see Goldberg, 1961, Theorem 5C) and evaluation at $l = l^*$ satisfying (20) as proved next.

In order to maximize (18), we need its derivative. By conditioning,

$$\mathrm{LB}(l) = \frac{e^{-rT}}{n+1}\sum_{j=0}^{n} E\left[E\left(S_{\tau+j\delta}-K\left|\frac{\sum_{j=0}^{n}\ln S_{\tau+j\delta}}{n+1}\right.\right)\mathbf{1}_{\left\{\frac{1}{n+1}\sum_{j=0}^{n}\ln S_{\tau+j\delta}>l\right\}}\right].$$

Taking the derivative with respect to l under the expectation sign gives

$$\begin{aligned}
\mathrm{LB}'(l) &= \frac{e^{-rT}}{n+1}\sum_{j=0}^{n} E\left[E\left(S_{\tau+j\delta}-K\left|\frac{\sum_{j=0}^{n}\ln S_{\tau+j\delta}}{n+1}\right.\right)\frac{d\mathbf{1}_{\left\{\frac{1}{n+1}\sum_{j=0}^{n}\ln S_{\tau+j\delta}>l\right\}}}{dl}\right] \\
&= \frac{-f(l)e^{-rT}}{n+1}\sum_{j=0}^{n} E\left(S_{\tau+j\delta}-K\left|\frac{\sum_{j=0}^{n}\ln S_{\tau+j\delta}}{n+1}=l\right.\right)
\end{aligned}$$

as the derivative of the function $x \mapsto \mathbf{1}_{\{x>0\}}$ is a Dirac function. f denotes the density function of $\sum_{j=0}^{n}\ln S_{\tau+j\delta}/(n+1)$. Then, the equation $\mathrm{LB}'(l^*) = 0$ gives

$$\sum_{j=0}^{n} E\left(S_{\tau+j\delta}\left|\frac{\sum_{j=0}^{n}\ln S_{\tau+j\delta}}{n+1}=l^*\right.\right) = K(n+1),$$

which, from Bartlett (1938, p. 62–63), can be rewritten in the form

$$\frac{\sum_{j=0}^{n}\int_{\mathbb{R}} e^{-il^*\upsilon}E\left[S_{\tau+j\delta}\exp\left(\frac{i\upsilon}{n+1}\sum_{j=0}^{n}\ln S_{\tau+j\delta}\right)\right]d\upsilon}{\int_{\mathbb{R}} e^{-il^*\upsilon}E\left[\exp\left(\frac{i\upsilon}{n+1}\sum_{j=0}^{n}\ln S_{\tau+j\delta}\right)\right]d\upsilon} = K(n+1).$$

(20) then follows from (16). This completes the proof. □

3 Data

We estimate the MR2JD model (1) on a panel dataset of freight options in the dry bulk market. We focus on average rate (Asian) option contracts that are traded on the BCI and BPI which are the most liquid. Baltic indices represent the cost of hiring a vessel across a range of indicative routes. BCI and BPI reflect freight market conditions in capesize and panamax vessels, i.e., the two largest in size classes of vessels transporting dry bulk commodities[3]. As a benchmark for the level of spot freight rates, the market uses the trip-charter route average (4TC); Table 1 shows the relevant composition for the BCI and BPI, respectively.

[INSERT TABLE 1]

Our dataset comprises Baltic Options Assessments (BOAs) of implied volatilities from at-the-money options (strikes equal to the prevailing FFA rates) that are submitted by freight option brokers to the Baltic Exchange. Our sample covers 336 weeks (every Friday) from 4 January 2008 to 6 June 2014. In line with market practice, we retrieve the market quotes from the implied volatilities every week using the option pricing formula of Turnbull and Wakeman (1991) and Levy (1997) (based on discrete averaging). The market quotes are for freight call options on the BCI and BPI that expire in the next four quarters (+1Q, +2Q, +3Q and +4Q) and the next two calendar years (+1CAL and +2CAL), which are the most common maturities. Each quarterly contract consists of 3 options that expire at the end of each month in the quarter of interest, whereas a calendar contract is a strip of 12 monthly options. This amounts to a total of 36 option prices available on each date in our sample, for each sector. For example, assume it is January 2010 and consider the +1Q contract: this comprises 3 freight options which settle at the end of each month in the following quarter, i.e., April, May and June 2010. The settlement prices of each of these options are given by the average of the spot rates over the trading days of the respective settlement month, i.e., commencement of averaging (e.g., beginning of April or May or June) does not coincide with the options' inception in January (forward start options, see Section 2.3). Similarly, the +1CAL

[3]Capesize vessels transport iron ore mainly from South America and Australia to the Far East (primarily China), and coal from North America, Australia and South Africa to the Far East and North Europe. The name is attributed to the fact that this type of vessel is too large to transit the Panama canal, therefore it has to navigate around Cape Horn. Panamax vessels are used mainly to carry grains from North America, Argentina and Australia, and coal from North America, Australia and South Africa either to Europe or the Far East. This is the largest permissible vessel size that can transit the Panama canal fully laden.

contract comprises 12 freight options which settle at the end of each consecutive calendar month in the following year, i.e., 2011 in this example.

4 Estimation

Model calibration is performed to option data for each sector. To this end, we resort to standard practice for extracting parameters from observed option prices. More specifically, let C^M_{w,T_i} be the market price in week $w = 1, \ldots, 336$ of the sample period (4 January 2008–6 June 2014) of an option maturing at T_i, $i = 1, \ldots, 36$, and C^θ_{w,T_i} the theoretical option price under the (log) spot rate model (1) with parameter vector $\theta := \{k_1, \varepsilon, \sigma, Y_0, k_2, \lambda, \mu_J, \sigma_J\}$. Theoretical option prices are given from (19).[4] We estimate θ every week w by minimizing the distance

$$\theta^*_w := \arg\min_\theta \sum_{i=1}^{36} \left| C^M_{w,T_i} - C^\theta_{w,T_i} \right|^2. \tag{21}$$

As a proxy for the risk free rate in our computations, we use the average 3-month US T-bill rate throughout the sample period.

5 Model validation

We begin our analysis with a discussion of the estimation results for the MR2JD model, for each of the dry bulk sectors. We then test the performance of the spot model in freight options pricing and analyze the errors. Finally, we examine the differences of the option prices produced by the suggested model as well as nested specifications (see Section 2.1).

5.1 Analysis of estimation results

In Table 2, we report the averages of the implied MR2JD model parameter estimates obtained weekly over the sample period, along with their standard errors; the reports are comparable for the two dry bulk sectors, which is not surprising given the high correlation between the capesize and panamax sectors.

[4] Our optimal lower bound is very fast to compute (up to 5 seconds per price) and accurate: numerical comparisons against true (but time-consuming) Monte Carlo price estimates suggest accuracy of our approach of 4 decimal places. We feel that presenting detailed speed-accuracy comparisons is beyond the scope and nature of this paper, however we can make them available upon request.

[INSERT TABLE 2]

The parameters λ, μ_J and σ_J are of particular interest as they signify the existence of jumps and, therefore, drive the skewness and excess kurtosis. We find that jumps in the BCI are more frequent, i.e., expected 27.98 jumps per year (λ) for the BCI versus 18.37 for the BPI, with smaller standard deviation of the jump size (σ_J) 45.6% for the BCI versus 56.1% for the BPI. The mean jump sizes (μ_J) are, respectively, -12.5% and -19.8% for the BCI and BPI resulting in negative skewness. Still, σ_J are high compared to μ_J, hence freight rates are susceptible to both positive and negative jumps. Figure 1 presents plots of the BCI and BPI log-returns sampled daily, along with ± 3 standard deviations' bounds. It clearly shows the discrepancy between the historical and normal distribution, corroborating the presence of jumps; it can be seen that spot freight rates entail more extreme movements than would be expected under a normal distribution. Moreover, the positive relationship between the jump arrival rate and the vessel size (confirmed also in Table 2) is not surprising, as smaller vessels are more versatile and can be employed to different routes mitigating large price swings. Occurrence of jumps in the freight markets is due to transitory imbalances in supply and demand curves for ocean shipping. When the supply and demand schedules are tight and the fleet is fully utilized, demand shocks lead to large price fluctuations as supply is unable to respond immediately. Changes in market expectations, or even unanticipated macroeconomic events, may contribute to abrupt price movements. For example, this was the case in the 2008 recession which led to fleet being unable to secure employment due to decreased demand for seaborne transportation. When freight rates fell to unprecedented low levels, shipowners preferred to make their ships available, even at bunker fuel costs, rather than laying them up and paying the cost of insurance.

[INSERT FIGURE 1]

Another item of note is that of mean-reversion in the stochastic process of freight rates. Several authors (inter alios, Bessembinder et al., 1995, Schwartz and Smith, 2000) have considered the effects of mean-reversion and argued that these models are more appropriate for commodities. In the shipping markets, intuitively, high freight rates encourage investment, leading to new vessels entering the market and, hence, increasing the supply of seaborne transportation that puts a downward pressure to freight rates in the long run[5]. Conversely, low rates lead to divestment,

[5]In the short run, supply is very inelastic as it is not possible to realize the effect of investing in new vessels due

causing supply decline. For example, when freight rates are close to, or even lower than operating expenses, laying up vessels and scrapping puts an upward pressure to prices. All things considered, freight may temporarily be high or low but with a tendency towards an equilibrium level. From (1), the log-spot freight rate is driven by two stationary processes: a mean-reverting diffusion X and jump process Y with different rates of reversion towards different levels. This type of mean-reversion in the freight rates arises from the market dynamics and reflects the distinctive self-adjustment behaviour in tight and ordinary supply-demand patterns. Rate k_1 implies that the expected time for X to return half way towards ε is slightly above 5.5 months for both sectors (half-life defined as $k^{-1} \ln 2$); shocks of the factor Y governing the jumps dissipate at rate k_2 with a half-life of marginally above 2 months. This is one of the important features of this model as jumps typically retract faster than the diffusion component.

[INSERT FIGURE 2]

The left graphs in Figure 2 show some example probabilistic forecasts (expected spot) generated by the model based on the parameters in Table 2. Initial spot prices are 34,732 and 19,724 USD for the BCI and BPI, respectively, given by the average weekly freight rates in the sample period. The solid lines in the left graphs represent forecasts for spot prices, whereas the dotted lines label the confidence bands for each index: we can see that the spot price is expected to drop towards the equilibrium level in nearly 6 months ahead. Sample paths of the spot freight rate under the MR2JD model are shown in the right graphs. It is worth noting the extreme price changes and their relatively quick reversion to equilibrium as, based on our model setup, these deviations should not last for a lengthy period of time.

[INSERT FIGURE 3]

To provide a more general idea of how the speed of adjustment coefficients affect the stochastic evolution of the freight rate, we show in Figure 3 the above probabilistic forecasts for different time horizons by perturbing k_1 and k_2 from their original values so that the half-lives become equal to 1 month and 1 year, with the remaining parameters unchanged. The dotted line represents the reference case based on the parameter values in Table 2. It is clear from Figure 3 that MR2JD can

to construction lags of 2–3 years (time to build). Nevertheless, higher speeds, reduced port times, shorter ballast legs and delayed regular maintenance are possible ways of increasing supply in the short run.

generate various shapes of expected spot curves (including hump shapes, Z-shapes, and tortuous curves), which can be directly linked to the term structure of FFAs via Eq. (8).

[INSERT FIGURE 4]

We conclude this section by presenting in Figure 4 the weekly evolutions of the implied cumulants (scaled where indicated) of the estimated MR2JD model for 1-month, 6-month and 12-month log-changes in the BCI (left) and BPI (right) given by Eqs. (3)–(7). The skewness coefficient is negative due to negative mean jump size. Increasing the time scale results in higher volatility, whereas the excess kurtosis and skewness coefficient approach zero.

5.2 Option pricing performance

In what follows, we study the empirical accuracy of the MR2JD model-implied option prices. To this end, we consider three key performance measures: mean absolute percentage error (MAPE), root mean square percentage error (RMSPE), and root mean square error (RMSE) in monetary terms,

$$\text{MAPE} = \frac{1}{nm}\sum_{w=1}^{n}\sum_{i=1}^{m}\left|\frac{C_{w,T_i}^{\theta_w^*}}{C_{w,T_i}^{M}}-1\right|, \tag{22}$$

$$\text{RMSPE} = \sqrt{\frac{1}{nm}\sum_{w=1}^{n}\sum_{i=1}^{m}\left|\frac{C_{w,T_i}^{\theta_w^*}}{C_{w,T_i}^{M}}-1\right|^2}, \tag{23}$$

$$\$\ \text{RMSE} = \sqrt{\frac{1}{nm}\sum_{w=1}^{n}\sum_{i=1}^{m}\left|C_{w,T_i}^{M}-C_{w,T_i}^{\theta_w^*}\right|^2}, \tag{24}$$

where $n = 336$ is the number of weeks in the sample period, m the number of option maturities and θ_w^* is given by (21). The performance measures (22)–(24) are reported in Table 3 for each index and have been calculated on the whole set of option prices ("All") as well as the three maturity-partitioned datasets: short-term (+Q encompassing the quarterly contracts altogether, i.e., +1Q, +2Q, +3Q, +4Q), medium-term (+1CAL), and long-term (+2CAL) options. For comparison purposes, we also consider the basic LGN model (see Section 2.1) which is favoured by global leaders in dry bulk derivatives, such as Freight Investor Services (FIS), and which we calibrate similarly.

[INSERT TABLE 3]

We first examine the pricing accuracy of the model based on the in-sample ("is") fit (goodness-of-fit of option pricing model, i.e., minimized distance 21). Our results suggest that MR2JD produces lower pricing errors than LGN. More specifically, for the BCI, the "All" RMSPE (MAPE) under MR2JD is 12.04% (8.50%). The "maturity-partitioned" RMSPE (MAPE) is 5.99–15.49% (4.89–12.97%), noting that the error magnitude declines for longer-term contracts. Similar are the results for the BPI with a "All" RMSPE (MAPE) of 10.23% (7.44%) and "maturity-partitioned" RMSPE (MAPE) of 5.44–13.13% (4.35–10.93%). Also, the fitted BCI MR2JD model yields an average $ RMSE of 387 USD which is higher than the BPI $ RMSE close to 176 USD. This can be attributed to the more volatile and prone to jumps BCI, as implied by our parameter estimates and based on our discussion in Section 5.1. Compared to the fitted LGN model, errors are 35–50% lower in USD terms.

Models that do well in in-sample estimation do not necessarily remain superior in out-of-sample ("oos") forecasting. For this, we turn next to the out-of-sample comparison: Table 3 reports the performance measures for the prediction pricing errors, i.e., the differences between observed and model option prices calculated using previous week's estimated parameters as in Bakshi et al. (1997). Not surprisingly, the out-of-sample errors are higher than the in-sample errors: for example, the BCI and BPI $ RMSEs under MR2JD experience an increase by a factor of approx. 1.6. Nevertheless, our findings remain qualitatively similar, i.e., MR2JD generates lower errors than LGN (23–45% lower in USD terms).

To analyze the statistical significance of the previous results, the Hansen (2005) test is employed. In particular, we define loss function (LF) differentials between LGN and MR2JD based on the time series of the performance measures (22)–(24), i.e., $\mathrm{LF}_w = \mathrm{G}_{\mathrm{LGN},w} - \mathrm{G}_{\mathrm{MR2JD},w}$, $w = 1, \ldots, 336$, for each measure G (MAPE, RMSPE, $ RMSE). Then, by performing 10,000 bootstrap simulations[6], we test the null hypothesis H_0: $E(\mathrm{LF}) \leq 0$. Rejection of H_0 (at conventional significance levels indicated by an asterisk in Table 3) implies that LGN is outperformed by MR2JD, hence accurately modelling jumps and mean-reversion of the price dynamics yields significant improvements to both the fit and prediction of the freight option prices.

We conclude this analysis by referring to an additional error statistic, that is, the mean per-

[6]Simulations are implemented using the stationary bootstrap of Politis and Romano (1994); we refer to Sullivan et al. (1999, Appendix C) for more details.

centage error (MPE) which can be used to test for existence of systematic bias:

$$\text{MPE} = \frac{1}{nm} \sum_{w=1}^{n} \sum_{i=1}^{m} \left(\frac{C_{w,T_i}^{\theta_w^*}}{C_{w,T_i}^{M}} - 1 \right). \tag{25}$$

Using the bootstrap simulation procedure outlined above, we test the null hypothesis H_0: $E(\text{MPE}) = 0$. The outcome of the test suggests no evidence of MR2JD-related bias for the BCI (BPI) in the case of the +1CAL option dataset (+Q and +1CAL), as opposed to LGN where errors are unanimously biased. Although the in- and out-of-sample results of the "All" option dataset suggest positive bias, translating to overpricing, for both indices, the MPEs are smaller (in absolute value) for MR2JD.

5.3 Analysis of option pricing errors

In this section, we evaluate the pricing biases of the MR2JD and LGN models. To this end, we perform a regression analysis on the percentage pricing errors $\text{PE} = C_{t,T}^{\theta^*}/C_{t,T}^{M} - 1$ to examine whether different variables cause option-specific, market-specific and general market conditions-specific systematic biases. We estimate the following regression using ordinary least squares

$$\text{PE} = \alpha_0 + \alpha_1 T + \alpha_2 T^2 + \alpha_3 \hat{\sigma}_S + \alpha_4 \hat{s}_S + \alpha_5 \hat{\kappa}_S + \alpha_6 dy + u, \tag{26}$$

where T is the option time to maturity (option-specific), $\hat{\sigma}_S$, $\hat{s}_S$ and $\hat{\kappa}_S$ the 6-month rolling standard deviation, skewness coefficient and excess kurtosis of daily spot freight log-returns (market-specific), and dy the differential between the 30-year and 3-month US T-bill rates (general market conditions); T^2 is included as an explanatory variable for any non-linear time-to-maturity effects.

[INSERT TABLE 4]

We run the regression for the in-sample and out-of-sample pricing errors and report the results in Table 4. The standard errors of the estimated coefficients are adjusted according to the Newey and West (1987) heteroscedasticity consistent estimator and are given in $(\cdot)$. The estimates $\hat{\alpha}_1$ are negative in all regressions, while the estimates $\hat{\alpha}_2$ have reverse signs, suggesting that the error is a convex function of T (with the exception of the MR2JD "is" results). Positive (negative) signs of estimates $\hat{\alpha}_3$, $\hat{\alpha}_4$ and $\hat{\alpha}_5$ imply that the model tends to overstate (understate) the option

prices as $\hat{\sigma}_S$, $\hat{s}_S$ and $\hat{\kappa}_S$ increase. Finally, the yield differential movements appear to have a rather small effect on the pricing error as indicated by $\hat{\alpha}_6$. In general, all the estimated coefficients are much higher (in absolute value) for LGN suggesting that the impact of the examined factors on the pricing error is more significant if mean-reversion and jumps are ignored.

Furthermore, the MR2JD pricing biases are always lower: the adjusted R^2 for the BCI and BPI "is" ("oos") OLS are 0.351% and 0.609% (1.337% and 1.413%) for MR2JD against 10.46% and 12.84% (9.521% and 10.53%) for LGN. The F statistics and standard errors of the estimated coefficients in Table 4 further suggest that MR2JD remarkably reduces the bias (although still significant), implying robustness of the proposed model. In particular, the pricing errors induced by MR2JD have only some maturity- and yield differential-related biases but are statistically insensitive to standard deviation, skewness and excess kurtosis. On the contrary, LGN produces errors which are biased towards all independent variables. In summary, MR2JD is sufficiently rich and capable of providing a more realistic description of the true data generating process, hence delivering model option prices that are least prone to systematic errors.

5.4 Option model comparisons

Based on the calibration results obtained on the last trading day of the sample period, we evaluate options under different nested model specifications (LGN, MR, MRJ – see Section 2.1) in order to assess their impact on the option prices.

We consider Asian call options with daily monitoring (i.e., $n = 22$), 6 and 12 months to maturity, and different levels of moneyness: the strike price is set equal to 70, 80, ..., 130% of the prevailing FFA price on 6 June 2014 closest to the maturity of interest, i.e., 26,435 USD ($T = 0.5$) and 21,195 USD ($T = 1$) for the BCI, and 11,404 USD ($T = 0.5$) and 10,741 USD ($T = 1$) for the BPI. The risk free interest rate is fixed at 2% per annum. The MR2JD model for the BCI (BPI) has been calibrated to a set of 36 option prices, according to (21), at the close of the market on 6 June 2014 with reported BCI (BPI) spot price of 13,370 USD (5,838 USD). The estimated model parameters and cumulants are presented in Table 5. Given these, in the ensuing analysis the cumulants are fitted to calibrate LGN, MR, MRJ. The computed option prices are displayed in Table 5 with figures expressed in '000s USD.

[INSERT TABLE 5]

Several comments are in order. We find that MR2JD prices are lower than LGN and MR prices, i.e., not taking into account observed empirical properties, such as jumps and mean-reversion, leads to overstated option prices. Linking this to our analysis in Section 5.3, where the bias of the pricing errors was found mainly positive (see $\hat{\alpha}_0$ in Table 4), supports our overvaluation argument, at least when LGN is put to the test (LGN model bias is also statistically sensitive to skewness and kurtosis, see $\hat{\alpha}_4$ and $\hat{\alpha}_5$ in Table 4). This pattern can be attributed to the combined excess kurtosis and negative skewness effect of the (log) spot distribution. Also obvious is the effect of modelling relatively faster mean-reverting jumps resulting in further lower MR2JD prices than MRJ ones, hence choosing between MRJ and MR2JD plays a primary role in determining option prices. Differences across sectors are observed as well: for the BCI (BPI), the option price differences of MR2JD and LGN, MR, MRJ stand, respectively, at 733, 864, 285 USD (64, 96 and 34 USD) on average – BPI differences are smaller due to lower spot price on the calibration day.

Continuing our empirical investigations, we note the slightly higher sensitivity of the BPI option prices to strike price changes. More specifically, in the case of MR2JD, for $T = 0.5$ and $K/\text{FFA} = 1.3$ (0.7) the relative price of the BCI option with respect to the $K/\text{FFA} = 1$ option price is 91.9% (117.6%), i.e., changing from $K/\text{FFA} = 1.3$ to 0.7 increases the option price by a factor of 1.3. Looking at the BPI options, the relevant price ratios are 84.1% and 123.3%, implying a price increase by a factor of 1.5 when changing from $K/\text{FFA} = 1.3$ to 0.7.

[INSERT FIGURE 5]

Finally, to gain a further insight into the differences between the MR2JD and MRJ models, we examine how the model-implied option prices diverge as we change each of the 'reversion' parameters. In particular, we demonstrate the effect of possible market-specific changes by perturbing parameters k_1 and k_2 from their original values in Table 5 to obtain 121 pairs of parameter values and compute the corresponding prices of options with different maturities, $T = 0.5$ and 1. Figure 5 portrays the option price profiles under the hypothetical parameterizations for the BCI and BPI; the grey surfaces depict the option values under the MRJ model (hence, subject to changes of k_1 only), whereas the multicolored surfaces are the outcome of changing both k_1 and k_2 of the MR2JD model. The analysis that follows illustrates the flexibility offered by distinct reversion scales for the jump and diffusion components in producing relevant option price shapes under prevailing market conditions. We find that the two rates affect substantially the option prices, with the effect of k_1

being more pronounced in the case of the MRJ model. In particular, the option prices increase with the half-life, yet in a non-linear fashion. This is expected as the freight rates on the last day of our sample exceed their equilibrium levels, which translates to a temporary deviation, hence freight rates are expected to drop (which did happen as BCI, for example, lost approx. 48% from June to December 2014 and 67% from June 2014 to June 2015). When the freight rate exceeds the equilibrium level, the mean-reversion process dictates that supply will increase due to incentive to placing new orders and disincentive to scrapping old vessels (see discussion in Section 5.1). In the short run (as our hypothetical options expire at $T = 0.5$ and 1), the source of mean-reversion might arise from, among others, increased vessel utilization rates and optimized speeds, placing a downward pressure to freight. Under such market conditions, when mean-reversion is strong, an at-the-money call option is less likely to be eventually exercised. (The opposite would be expected if freight was below the equilibrium level.) Similar observations apply to the case of MR2JD, although the relationship between $k_1^{-1} \ln 2$ and the option price is less perceptible, while this becomes more profound as the jump component's half-life ($k_2^{-1} \ln 2$) increases. In our case, the option price is an increasing and concave function of $k_2^{-1} \ln 2$ due to negative mean jump size (see Table 5): negative jumps dissipating fast (slow) result in increasing (decreasing) call option prices (whereas positive jumps would, instead, have an opposite effect).

6 Conclusions

In this paper we study the MR2JD freight model with decoupled mean-reverting diffusive and jump components reflecting freight's distinctive self-adjustment behaviour under tight and ordinary supply-demand patterns. We also develop an analytical solution for tradable average options in terms of characteristic functions under the postulated dynamics.

We calibrate the spot rate process to Baltic option price data and provide evidence of MR2JD's ability to describe flexibly the stochastic process for freight in the dry bulk sector. We find that jumps dissipate faster than diffusive deviations about the equilibrium level. The improvement in option pricing performance brought by MR2JD is illustrated by various error statistics and by comparing also with the traditional lognormal framework. MR2JD produces lower pricing errors by 35–50% (in USD terms); our results are confirmed by an out-of-sample exercise with the MR2JD errors lower by 23–45%. A regression analysis shows that MR2JD generates pricing errors with

least option-specific, market-specific and general market conditions-related biases, confirming its superior performance. Finally, we evaluate average options under nested model variants to assess the effects of different parameterizations on the option prices. Neglecting jumps and/or fast mean-reversion when jumps occur leads to overstated option prices; model risk is less severe when both ingredients are included.

The implications of this research are important for various stakeholders in the industry adding to their understanding of the freight market dynamics, as, for market participants, the main consideration is that the fair price of freight-related assets truly reflects the associated market risks. Our work is of potential interest to investors for evaluating their derivatives positions, assessing and comparing alternative investments, and hedging their exposures. We also believe that this research has potential and immediate applications to the practice of decision making. Analyzing the problem of vessel replacement and/or the decision to enter and exit the market using real options, given a certain depreciation policy and operating expenses process, are left for future research.

References

Adland, R., Cullinane, K., 2006. The non-linear dynamics of spot freight rates in tanker markets. Transportation Research Part E: Logistics and Transportation Review 42 (3), 211–224.

Alexandridis, G., Sahoo, S., Visvikis, I., 2017. Economic information transmissions and liquidity between shipping markets: New evidence from freight derivatives. Transportation Research Part E: Logistics and Transportation Review 98, 82–104.

Alizadeh, A. H., Kappou, K., Tsouknidis, D., Visvikis, I., 2015. Liquidity effects and FFA returns in the international shipping derivatives market. Transportation Research Part E: Logistics and Transportation Review 76, 58–75.

Bakshi, G., Cao, C., Chen, Z., 1997. Empirical performance of alternative option pricing models. The Journal of Finance 52 (5), 2003–2049.

Bartlett, M. S., 1938. The characteristic function of a conditional statistic. Journal of the London Mathematical Society 13 (1), 62–67.

Benth, F. E., Koekebakker, S., 2016. Stochastic modeling of Supramax spot and forward freight rates. Maritime Economics & Logistics 18 (4), 391–413.

Bessembinder, H., Coughenour, J. F., Seguin, P. J., Smoller, M. M., 1995. Mean reversion in equilibrium asset prices: Evidence from the futures term structure. The Journal of Finance 50 (1), 361–375.

Bjerksund, P., Ekern, S., 1995. Contingent claims evaluation of mean-reverting cash flows in shipping. In: Trigeorgis, L. (Ed.), Real Options in Capital Investment: Models, Strategies, and Applications. Praeger, Westport, pp. 207–219.

Bjørkelund, A. M., 2014. Pricing in offshore shipping markets: A two-regime mean reverting jump diffusion model with seasonality, Master thesis, Norwegian School of Economics.

Curran, M., 1994. Valuing Asian and portfolio options by conditioning on the geometric mean price. Management Science 40 (12), 1705–1711.

Fusai, G., Kyriakou, I., 2016. General optimized lower and upper bounds for discrete and continuous arithmetic Asian options. Mathematics of Operations Research 41 (2), 531–559.

Geman, H., Roncoroni, A., 2006. Understanding the fine structure of electricity prices. The Journal of Business 79 (3), 1225–1261.

Geman, H., Smith, W. O., 2012. Shipping markets and freight rates: An analysis of the Baltic Dry Index. The Journal of Alternative Investments 15 (1), 98–109.

Goldberg, R. R., 1961. Fourier Transforms. Cambridge Tracts in Mathematics and Mathematical Physics, No. 52. Cambridge University Press, Cambridge.

Greenwood, R., Hanson, S. G., 2015. Waves in ship prices and investment. Quarterly Journal of Economics 130 (1), 55–109.

Hansen, P. R., 2005. A test for superior predictive ability. Journal of Business & Economic Statistics 23 (4), 365–380.

Hikspoors, S., Jaimungal, S., 2007. Energy spot price models and spread options pricing. International Journal of Theoretical and Applied Finance 10 (7), 1111–1135.

Jørgensen, P. L., De Giovanni, D., 2010. Time charters with purchase options in shipping: Valuation and risk management. Applied Mathematical Finance 17 (5), 399–430.

Kalouptsidi, M., 2014. Time to build and fluctuations in bulk shipping. The American Economic Review 104 (2), 564–608.

Kavussanos, M. G., Visvikis, I. D., 2004. Market interactions in returns and volatilities between spot and forward shipping freight markets. Journal of Banking & Finance 28 (8), 2015–2049.

Kavussanos, M. G., Visvikis, I. D., 2006. Shipping freight derivatives: a survey of recent evidence. Maritime Policy & Management 33 (3), 233–255.

Kavussanos, M. G., Visvikis, I. D., Dimitrakopoulos, D. N., 2014. Economic spillovers between related derivatives markets: The case of commodity and freight markets. Transportation Research Part E: Logistics and Transportation Review 68, 79–102.

Kilian, L., 2009. Not all oil price shocks are alike: Disentangling demand and supply shocks in the crude oil market. The American Economic Review 99 (3), 1053–1069.

Koekebakker, S., Adland, R., Sødal, S., 2006. Are spot freight rates stationary? Journal of Transport Economics and Policy 40 (3), 449–472.

Koekebakker, S., Adland, R., Sødal, S., 2007. Pricing freight rate options. Transportation Research Part E: Logistics and Transportation Review 43 (5), 535–548.

Levy, E., 1997. Asian options. In: Clewlow, L., Strickland, C. (Eds.), Exotic Options: The State of the Art. International Thomson Business Press, Washington DC, pp. 65–91.

Newey, W. K., West, K. D., 1987. A simple, positive semi-definite, heteroskedasticity and autocorrelation consistent covariance matrix. Econometrica 55 (3), 703–708.

Nomikos, N. K., Kyriakou, I., Papapostolou, N. C., Pouliasis, P. K., 2013. Freight options: Price modelling and empirical analysis. Transportation Research Part E: Logistics and Transportation Review 51, 82–94.

Nomikos, N. K., Soldatos, O., 2008. Using affine jump diffusion models for modelling and pricing electricity derivatives. Applied Mathematical Finance 15 (1), 41–71.

Papapostolou, N. C., Nomikos, N. K., Pouliasis, P. K., Kyriakou, I., 2014. Investor sentiment for real assets: the case of dry bulk shipping market. Review of Finance 18 (4), 1507–1539.

Politis, D. N., Romano, J. P., 1994. The stationary bootstrap. Journal of the American Statistical Association 89 (428), 1303–1313.

Prokopczuk, M., 2011. Pricing and hedging in the freight futures market. Journal of Futures Markets 31 (5), 440–464.

Rogers, L. C. G., Shi, Z., 1995. The value of an Asian option. Journal of Applied Probability 32 (4), 1077–1088.

Schwartz, E., Smith, J. E., 2000. Short-term variations and long-term dynamics in commodity prices. Management Science 46 (7), 893–911.

Schwartz, E. S., 1997. The stochastic behaviour of commodity prices: Implications for valuation and hedging. The Journal of Finance 52 (3), 923–973.

Sullivan, R., Timmermann, A., White, H., 1999. Data-snooping, technical trading rule performance, and the bootstrap. The Journal of Finance 54 (5), 1647–1691.

Turnbull, S. M., Wakeman, L. M., 1991. A quick algorithm for pricing European average options. Journal of Financial and Quantitative Analysis 26, 377–389.

Tvedt, J., 1997. Valuation of VLCCs under income uncertainty. Maritime Policy & Management 24 (2), 159–174.

Tvedt, J., 2003. Shipping market models and the specification of freight rate processes. Maritime Economics & Logistics 5 (4), 327–346.

Zannetos, Z. S., 1966. The Theory of Oil Tankship Rates: An Economic Analysis of Tankship Operations. MIT Press, Cambridge, Massachusetts.

Table 1: Composition of trip-charter routes of Baltic indices

Route	Route description
Baltic Capesize Index	
C8	Delivery Gibraltar–Hamburg range for a Trans-Atlantic round voyage
C9	Delivery ARA–Mediterranean range for a trip to the Far East, redelivery China–Japan range
C10	Delivery China–Japan for a Pacific round voyage, redelivery China–Japan range
C11	Delivery China–Japan range for a trip to ARA or the Mediterranean
Baltic Panamax Index	
P1A	Delivery Gibraltar–Hamburg range for a Trans-Atlantic round voyage
P2A	Delivery Cape Skaw–Gibraltar range for a trip to the Far East (Japan–S. Korea range) via US Gulf
P3A	Delivery Japan–S. Korea for a Trans-Pacific round voyage
P4A	Delivery Far East for a trip to Europe (Cape Skaw–Cape Passero) via North Pacific or Australia

Routes composing (equally-weighted) the Baltic Capesize and Panamax 4TC Indices as in January 2015. BCI routes C8–C11 are for a standard 172,000 metric tons (mt) deadweight (dwt) capesize vessel of not more than 10 years of age. BPI routes P1A–P4A are for a standard 74,000 mt dwt panamax vessel of not more than 12 years of age. (Source: www.balticexchange.com)

Table 2: Average MR2JD model-implied parameters

	ε	k_1	σ	k_2	λ	μ_J	σ_J	Y_0
Baltic Capesize Index								
estimate	2.963	1.504	1.661	3.833	27.98	-0.125	0.456	1.348
standard error	0.129	0.210	0.072	0.355	0.932	0.005	0.008	0.087
Baltic Panamax Index								
estimate	2.392	1.451	0.812	3.772	18.37	-0.198	0.561	1.180
standard error	0.087	0.186	0.059	0.298	0.806	0.010	0.001	0.052

MR2JD model calibration to BCI and BPI option prices every Friday in the period 4 January 2008–6 June 2014 (336 weeks) (see Eq. 21). Average (across weeks) annual parameters with standard errors reported.

Table 3: Option pricing errors

		MR2JD				LGN			
		MPE	MAPE	RMSPE	$ RMSE	MPE	MAPE	RMSPE	$ RMSE
Baltic Capesize Index									
is	All	0.98*	8.50*	12.04*	386.6*	-1.06*	27.26	37.17	1,048.9
	+Q	0.99	12.97*	15.49*	519.7*	7.20*	34.29	43.23	1,447.9
	+1CAL	-0.65	8.04*	10.26*	361.4*	7.86*	25.75	33.82	707.1
	+2CAL	2.59*	4.89*	5.99*	218.8*	-17.41*	22.38	23.76	575.2
oos	All	2.58*	14.85*	19.28*	660.6*	3.07*	42.24	51.70	1,950.5
	+Q	3.50*	21.10*	24.99*	799.2*	11.06*	48.24	57.00	1,827.8
	+1CAL	1.05	14.34*	16.89*	568.2*	12.76*	43.52	51.66	1,693.3
	+2CAL	3.05*	9.68*	10.94*	411.6*	-13.97*	35.40	36.96	1,805.4
Baltic Panamax Index									
is	All	0.69*	7.44*	10.23*	176.4*	4.98*	22.67	31.34	447.2
	+Q	-1.12	10.93*	13.13*	240.6*	11.27*	30.70	38.18	598.1
	+1CAL	0.98	7.36*	9.28*	145.2*	15.70*	22.05	29.20	322.5
	+2CAL	2.02*	4.35*	5.44*	118.5*	-11.25*	16.08	17.62	318.8
oos	All	1.84*	12.19*	16.11*	286.6*	6.28*	33.53	41.97	750.3
	+Q	0.90	17.47*	21.07*	338.9*	12.58*	40.72	47.71	760.5
	+1CAL	1.01	11.82*	14.34*	233.6*	17.06*	34.74	41.37	706.1
	+2CAL	3.06*	7.64*	8.81*	183.3*	-10.03*	26.00	27.85	677.7

BCI and BPI performance measures (22)–(25) obtained across 336 weeks in the sample period 4 January 2008–6 June 2014 based on: whole set of option prices ("All") and maturity-partitioned datasets (+Q (comprising +1Q, +2Q, +3Q, +4Q altogether), +1CAL, +2CAL options). Theoretical option prices (see Eq. 19) used in the computation of the measures every week are based on the parameter estimates every week of the MR2JD and LGN models. In-sample ("is") pricing errors correspond to the goodness-of-fit of each pricing model, i.e., the minimized distance (21). Out-of-sample ("oos") pricing errors correspond to the differences between observed and theoretical option prices calculated using previous week's parameter estimates. To test the null hypothesis that the MPE is equal to zero, we employ the stationary bootstrap of Politis and Romano (1994) with 10,000 bootstrap simulations. In addition, we test the null hypothesis of the MR2JD not performing better than the LGN model, in terms of the MAPE, RMSPE and $ RMSE measures, by employing the reality check of Hansen (2005). Asterisk * indicates significance at conventional levels.

Table 4: Regression analysis of pricing errors

	is		oos	
	MR2JD	LGN	MR2JD	LGN
Baltic Capesize Index				
$\hat{\alpha}_0$	0.035*	0.524*	-0.052	0.493*
	(0.014)	(0.033)	(0.052)	(0.113)
$\hat{\alpha}_1$	-0.007	-0.665*	-0.086*	-0.657*
	(0.012)	(0.025)	(0.039)	(0.089)
$\hat{\alpha}_2$	-0.001	0.165*	0.044*	0.155*
	(0.004)	(0.008)	(0.013)	(0.027)
$\hat{\alpha}_3$	0.005	0.081*	0.005	0.207*
	(0.010)	(0.022)	(0.030)	(0.063)
$\hat{\alpha}_4$	-0.004*	0.008*	-0.005	0.090*
	(0.002)	(0.004)	(0.006)	(0.014)
$\hat{\alpha}_5$	-0.001421	-0.006*	-0.003	-0.013*
	(0.001)	(0.002)	(0.003)	(0.006)
$\hat{\alpha}_6$	-0.005*	-0.036*	0.021	-0.044*
	(0.003)	(0.008)	(0.013)	(0.026)
adj. R^2	0.351	10.46	1.337	9.521
Fstat.	7.896*	229.6*	27.68*	207.1*
Baltic Panamax Index				
$\hat{\alpha}_0$	0.039*	0.357*	0.024	0.147*
	(0.011)	(0.020)	(0.025)	(0.076)
$\hat{\alpha}_1$	-0.041*	-0.283*	-0.080*	-0.281*
	(0.010)	(0.019)	(0.024)	(0.067)
$\hat{\alpha}_2$	0.011*	0.033*	0.022*	0.030
	(0.003)	(0.007)	(0.007)	(0.020)
$\hat{\alpha}_3$	-0.006	-0.059*	0.028	0.203*
	(0.007)	(0.019)	(0.031)	(0.072)
$\hat{\alpha}_4$	0.001	0.030*	0.006	0.126*
	(0.003)	(0.006)	(0.010)	(0.019)
$\hat{\alpha}_5$	-0.001	-0.015*	0.010	-0.015*
	(0.002)	(0.003)	(0.010)	(0.007)
$\hat{\alpha}_6$	-0.001	0.007*	0.012*	0.040*
	(0.003)	(0.005)	(0.007)	(0.018)
adj. R^2	0.609	12.84	1.413	10.53
Fstat.	13.11*	292.1*	29.24*	231.7*

Coefficient estimates of regression (26) for in-sample ("is") and out-of-sample pricing errors ("oos"), for MR2JD and LGN models. Heteroscedasticity robust standard errors reported in $(\cdot)$. F statistics (Fstat.) and adjusted (adj.) R^2 (%) also reported. Asterisk * indicates significance at conventional levels.

Table 5: Option model comparisons

T	K/FFA	LGN	MR	MRJ	MR2JD
Baltic Capesize Index					
MR2JD *parameters*: $\varepsilon = 0.315$, $k_1 = 0.412$, $\sigma = 3.273$,					
$k_2 = 1.151$, $\lambda = 25.27$, μ_J = -0.243, $\sigma_J = 0.397$, $Y_0 = 3.362$					
Cumulants: c_1 = -1.016, $c_2 = 6.017$, $c_3 c_2^{-3/2}$ = -0.053, $c_4 c_2^{-2} = 0.018$					
0.5	0.7	4.813	4.940	4.312	4.061
0.5	0.8	4.659	4.784	4.158	3.915
0.5	0.9	4.520	4.645	4.020	3.784
0.5	1.0	4.395	4.519	3.896	3.667
0.5	1.1	4.281	4.403	3.783	3.560
0.5	1.2	4.176	4.297	3.679	3.462
0.5	1.3	4.079	4.199	3.584	3.371
Cumulants: c_1 = -2.996, $c_2 = 9.439$, $c_3 c_2^{-3/2}$ = -0.032, $c_4 c_2^{-2} = 0.008$					
1.0	0.7	4.503	4.644	4.107	3.754
1.0	0.8	4.433	4.573	4.036	3.688
1.0	0.9	4.369	4.509	3.972	3.629
1.0	1.0	4.310	4.449	3.913	3.574
1.0	1.1	4.256	4.395	3.859	3.523
1.0	1.2	4.206	4.344	3.808	3.476
1.0	1.3	4.158	4.296	3.761	3.432
Baltic Panamax Index					
MR2JD *parameters*: ε = -0.865, $k_1 = 1.006$, $\sigma = 2.746$,					
$k_2 = 3.038$, $\lambda = 14.07$, μ_J = -0.116, $\sigma_J = 0.502$, $Y_0 = 1.672$					
Cumulants: c_1 = -0.340, $c_2 = 2.963$, $c_3 c_2^{-3/2}$ = -0.027, $c_4 c_2^{-2} = 0.028$					
0.5	0.7	1.281	1.323	1.251	1.211
0.5	0.8	1.189	1.231	1.160	1.123
0.5	0.9	1.110	1.151	1.082	1.048
0.5	1.0	1.041	1.081	1.014	0.982
0.5	1.1	0.980	1.019	0.953	0.924
0.5	1.2	0.926	0.963	0.900	0.872
0.5	1.3	0.877	0.914	0.852	0.826
Cumulants: c_1 = -0.947, $c_2 = 3.860$, $c_3 c_2^{-3/2}$ = -0.018, $c_4 c_2^{-2} = 0.016$					
1.0	0.7	1.291	1.317	1.257	1.217
1.0	0.8	1.222	1.248	1.190	1.151
1.0	0.9	1.162	1.187	1.130	1.093
1.0	1.0	1.109	1.134	1.077	1.042
1.0	1.1	1.061	1.086	1.030	0.996
1.0	1.2	1.018	1.042	0.987	0.955
1.0	1.3	0.979	1.002	0.949	0.917

MR2JD-implied prices ('000s USD) of arithmetic average freight call options with maturity time T (years), $n = 22$ monitoring dates, FFA = 26,435 ($T = 0.5$), 21,195 USD ($T = 1.0$) for the BCI, 11,404 ($T = 0.5$), 10,741 USD ($T = 1$) for the BPI (as on last day of our sample, i.e., 6 June 2014), and K/FFA = $70, 80, \ldots, 130\%$. Initial spot freight rates as on 6 June 2014: 13,370 (5,838 USD) for the BCI (BPI). Model parameters: calibration to BCI and BPI option prices on 6 June 2014 (see table above). Risk free interest rate: 2% p.a. Also reported for comparison purposes LGN, MR and MRJ-implied option prices (model parameters obtained by matching to MR2JD cumulants, see Eqs. 3–7, reported in table above).

Figure 1

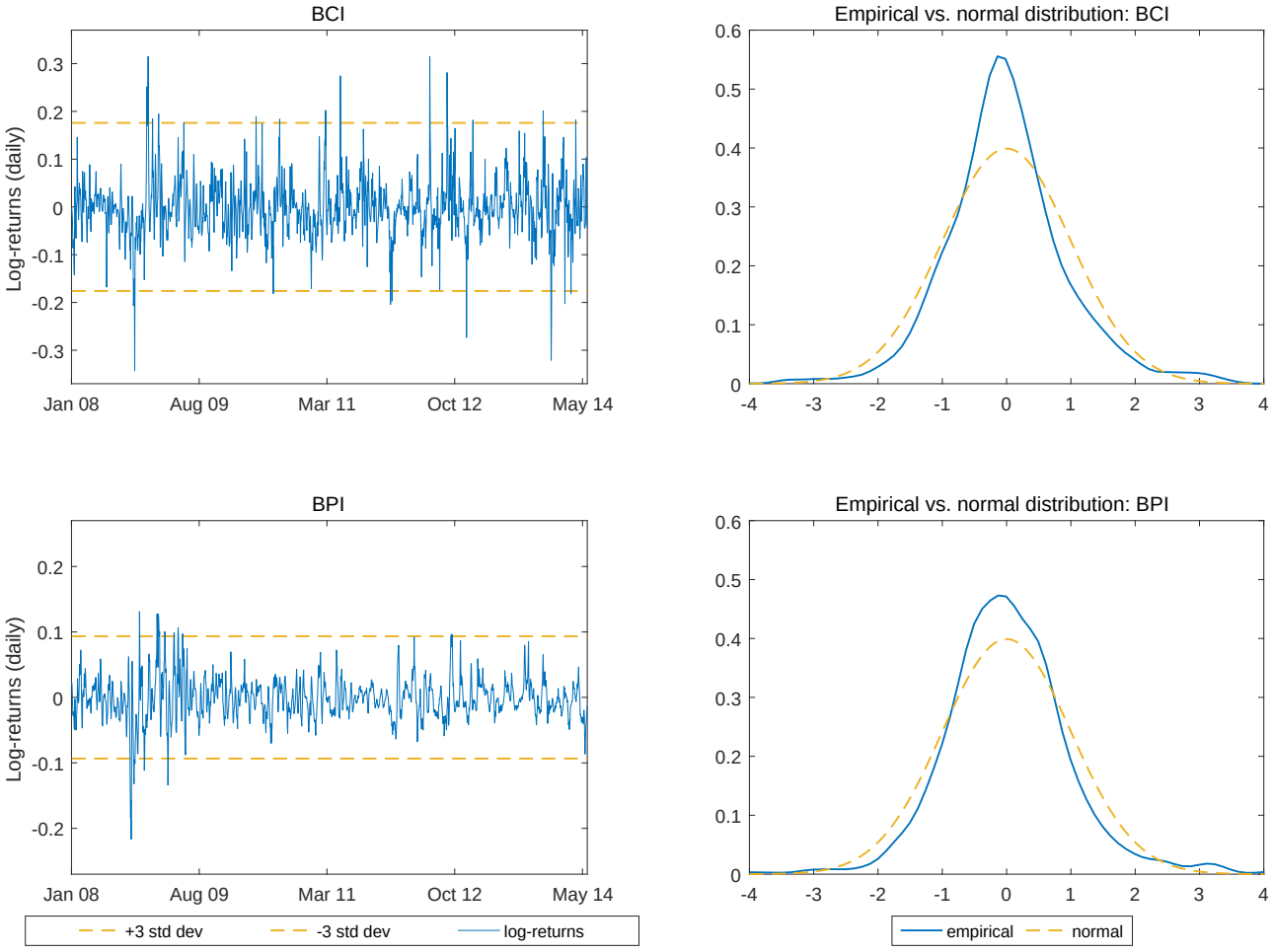

Left: Daily BCI and BPI log-returns 4 January 2008–6 June 2014. Right: Probability densities (Matlab's kernel smoothing function estimates) of standardized log-returns against standard normal distribution.

Figure 2

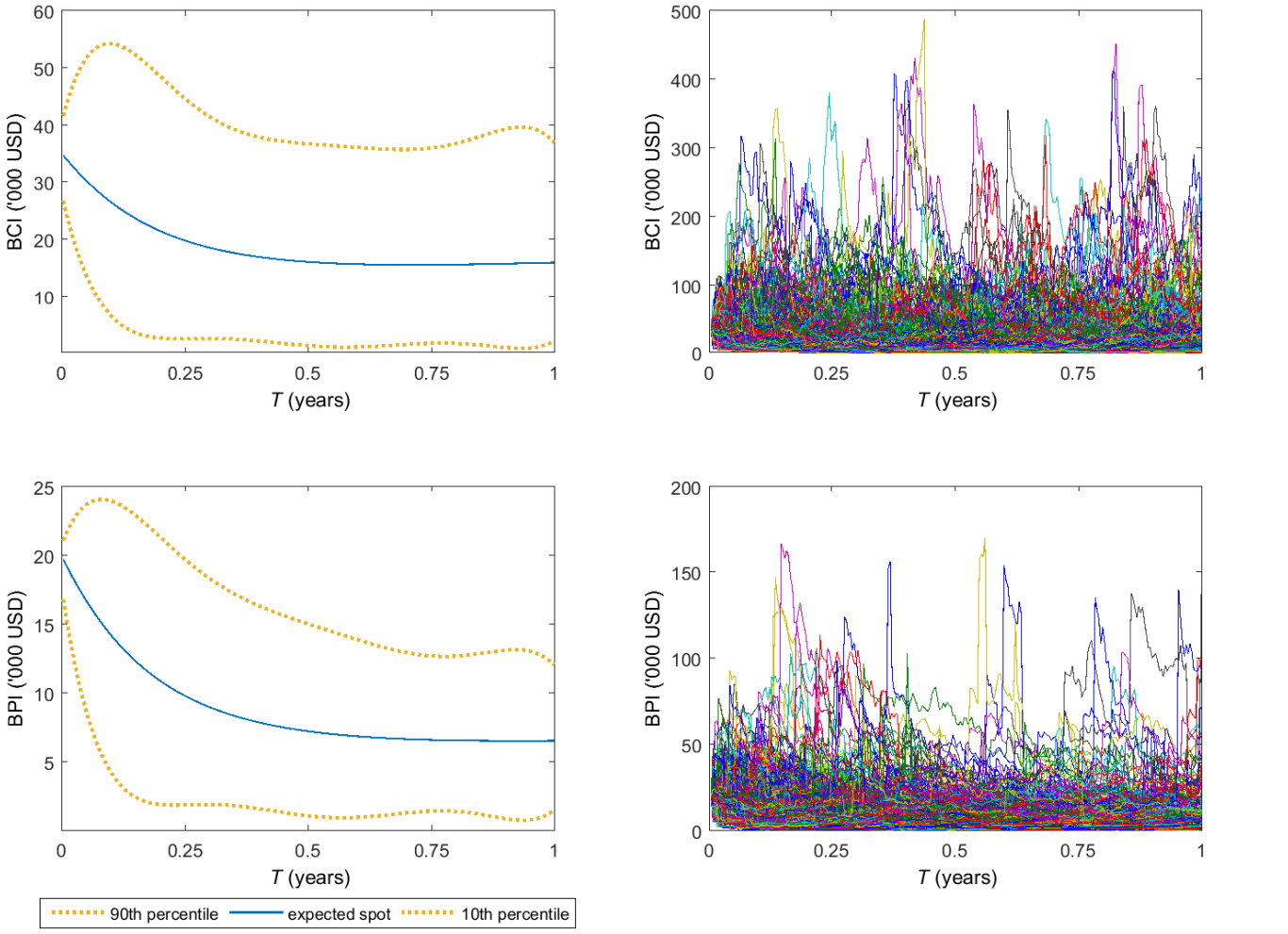

Left: Example probabilistic forecasts generated by the MR2JD model. Initial spot prices: 34,732 (19,724 USD) for the BCI (BPI). Model parameters: Table 2. Central solid lines: forecasts for spot prices (expected value forecasts). Upper and lower dotted lines: "confidence bands" corresponding to a 90% and a 10% chance that freight will be below those levels in the period ahead. Right: MR2JD spot freight rate sample paths.

Figure 3

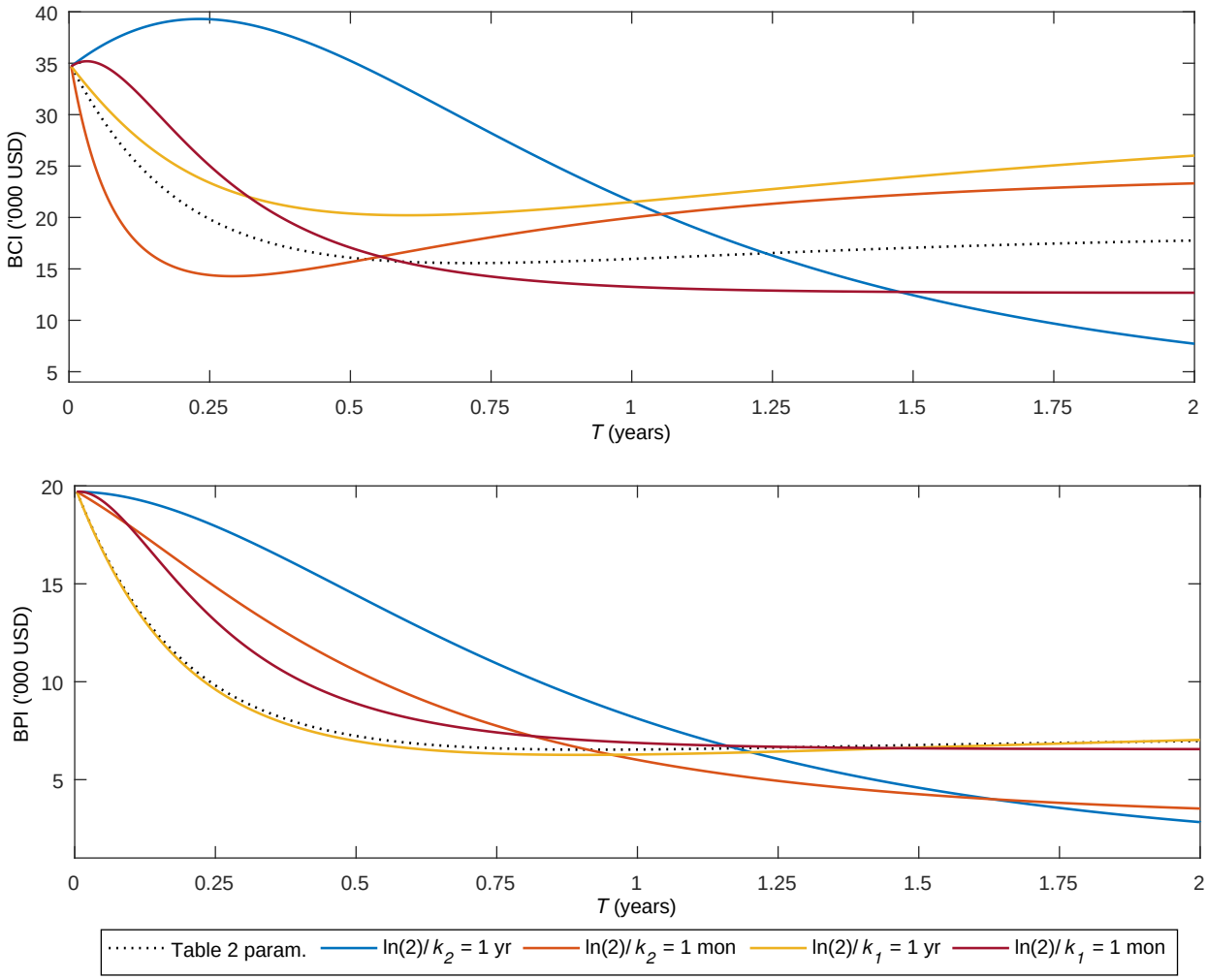

Expected spot freight evolution for different speeds of mean-reversion (k_1 and k_2), equivalently half-lives ($\ln(2)/k_1$ and $\ln(2)/k_1$), of the MR2JD model. Initial spot prices: 34,732 (19,724 USD) for the BCI (BPI). Other model parameters: Table 2.

Figure 4

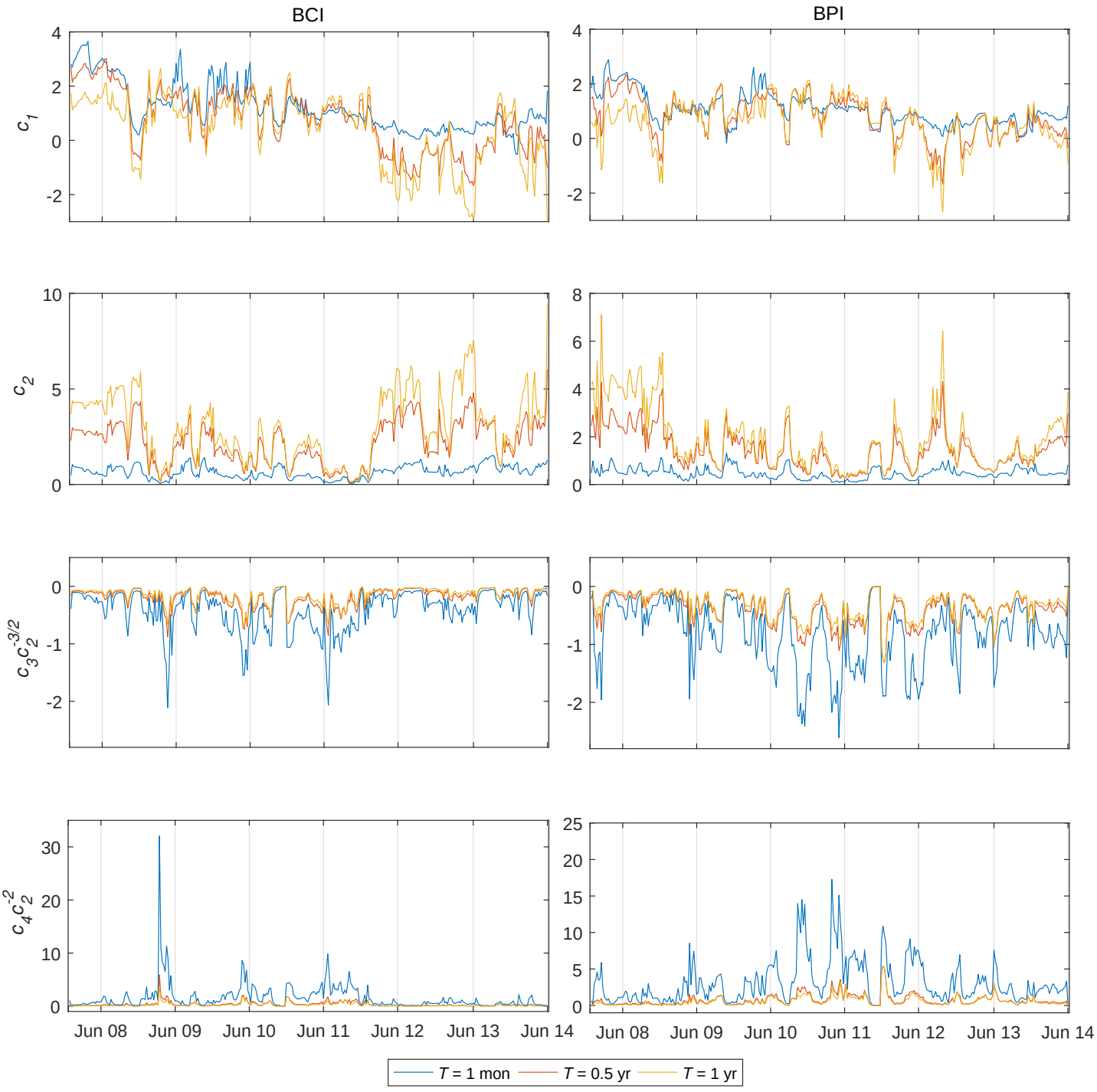

Weekly MR2JD (scaled where indicated) cumulants (3)–(7) based on parameter estimates from calibration to BCI and BPI option prices every Friday in the period 4 January 2008–6 June 2014 (see Eq. 21).

Figure 5

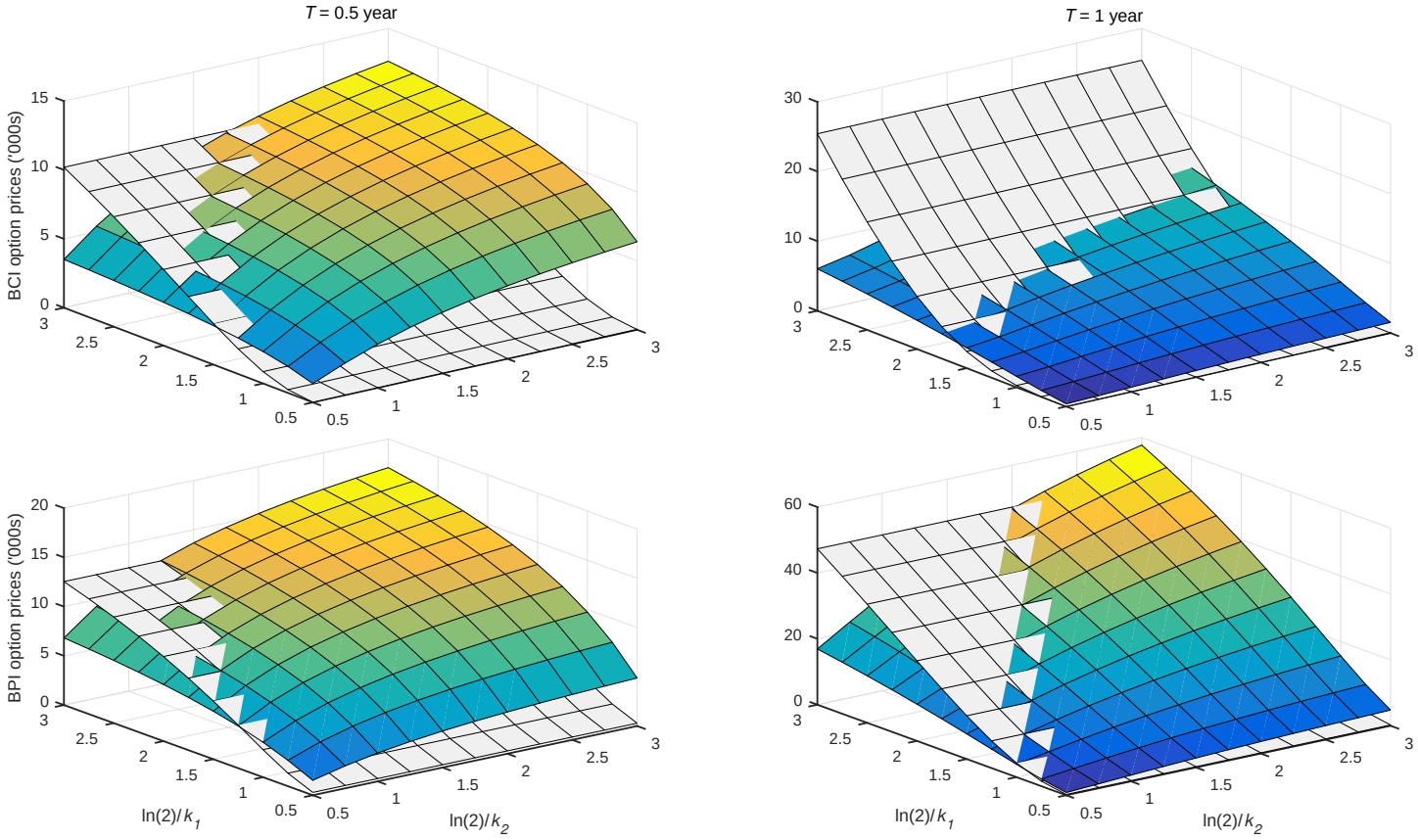

Multicolored surfaces: Effects of changing half-lives ($\ln(2)/k_1$ and $\ln(2)/k_1$) on the MR2JD-implied price of the arithmetic average freight call option with maturity time T (years), $n = 22$ monitoring dates, FFA = 26, 435 ($T = 0.5$), 21, 195 USD ($T = 1.0$) for the BCI, 11, 404 ($T = 0.5$), 10, 741 USD ($T = 1$) for the BPI (as on last day of our sample, i.e., 6 June 2014), and $K/\text{FFA} = 1$. Initial spot freight rates as on 6 June 2014: 13,370 (5,838 USD) for the BCI (BPI). Other model parameters: calibration to BCI and BPI option prices on 6 June 2014 (see Table 5). Risk free interest rate: 2% p.a. Grey surfaces: MRJ-implied option prices provided for comparison purposes (MRJ parameters obtained by matching to MR2JD cumulants, see Eqs. 3–7).